How to cite: *Angew. Chem. Int. Ed.* **2023,** *62,* e202217252
International Edition: doi.org/10.1002/anie.202217252
German Edition: doi.org/10.1002/ange.202217252

CO Reduction

Enhanced Carbon Monoxide Electroreduction to $>1\ A\,cm^{-2}$ C_{2+} Products Using Copper Catalysts Dispersed on MgAl Layered Double Hydroxide Nanosheet House-of-Cards Scaffolds

*Sunglun Kwon, Jie Zhang, Ramesha Ganganahalli, Sumit Verma, and Boon Siang Yeo**

Abstract: Cu catalysts are most apt for reducing $CO_{(2)}$ to multi-carbon products in aqueous electrolytes. To enhance the product yield, we can increase the overpotential and the catalyst mass loading. However, these approaches can cause inadequate mass transport of $CO_{(2)}$ to the catalytic sites, which will then lead to H_2 evolution dominating the product selectivity. Herein, we use a MgAl LDH nanosheet 'house-of-cards' scaffold to disperse CuO-derived Cu (OD-Cu). With this support-catalyst design, at $-0.7\ V_{RHE}$, CO could be reduced to C_{2+} products with a current density (j_{C2+}) of $-1251\ mA\,cm^{-2}$. This is 14× that of the j_{C2+} shown by unsupported OD-Cu. The current densities of C_{2+} alcohols and C_2H_4 were also high at −369 and $-816\ mA\,cm^{-2}$ respectively. We propose that the porosity of the LDH nanosheet scaffold enhances CO diffusion through the Cu sites. The CO reduction rate can thus be increased, while minimizing H_2 evolution, even when high catalyst loadings and large overpotentials are used.

Introduction

The electrocatalytic CO_2 or CO reduction reaction (CO_2RR or CORR) in aqueous electrolytes, powered by renewable electricity, has drawn attention in recent years as a sustainable approach to produce green fuels and chemical feedstocks.[1–3] In order to scale up this process for widespread deployment, it is necessary to enhance the yield (current densities) of products formed.[2,4] The most direct way to achieve this would be to increase the catalyst mass loading on the electrode. However, this practice can lead to an unwanted agglomeration of the catalyst particles.[4,5] As such, catalyst mass loadings are often kept to $<2\ mg\,cm^{-2}$.[2,4–6] To prevent agglomeration of catalyst particles, supports such as high surface area graphene or carbon nanotubes can be used.[7,8] Unfortunately, trace metal impurities, known to be present on these carbon materials, can alter the properties of the catalysts, or worse still, poison and catalytically deactivate them.[9–11] Another method to increase the reaction yield is to apply a larger overpotential. These commonly used approaches have a major drawback: As the reaction rate per geometric surface area of the electrode increases, the CO_2 or CO feedstock may percolate insufficiently into the catalyst layer.[2,5,7] Consequently, the parasitic hydrogen evolution reaction (HER) will start to dominate the selectivity of products formed. For this reason, considerable efforts have been devoted to understanding changes in the structures and properties of catalyst films as a function of its composition, and the effect of these changes on the rate and selectivity of CO_2 or CO reduction.

An alternative catalyst support is layered double hydroxides (LDH). The general formula of LDH is $[M^{2+}_{(1-x)}M^{3+}_{x}(OH)_2]A^{n-}_{(x/n)}\cdot mH_2O$, where M^{2+} and M^{3+} are the divalent and trivalent metal ions respectively, and A^{n-} is the intercalating anion.[12,13] LDH nanoparticles can also be exfoliated to high surface area nanosheets.[14–16] A property of the LDH nanoparticles or nanosheets is that as the number of their surface atoms relative to bulk atoms increases, the surface-to-surface attraction between the particles is enhanced.[17] Continuous films made up of LDH nanoparticles/nanosheets can thus be formed, exhibiting structures that resemble 'house-of-cards'.[17,18] We envisage that these structures can serve as scaffolds to disperse the catalysts (Figure 1a–b). The resulting porosity in the catalyst layer will thus allow better CO or CO_2 gas penetration.

On the basis of the above discussion, we demonstrate herein the use of a house-of-cards scaffold made of MgAl LDH nanosheets to support CuO-derived Cu (OD-Cu) catalysts for CORR. The MgAl LDH nanosheet house-of-cards structure was effective in dispersing the OD-Cu nanoparticles during CORR. Together, they also reduced CO to C_{2+} products with high activity and selectivity. Using this system, C_{2+} products could be formed at −0.7 V vs.

[*] Dr. S. Kwon, Dr. J. Zhang, Prof. Dr. B. S. Yeo
Department of Chemistry, Faculty of Science, National University of Singapore
3 Science Drive 3, 117543 Singapore (Singapore)
E-mail: chmyeos@nus.edu.sg
Dr. R. Ganganahalli
Shell India Markets Private LTD Plot No. 7,
Bengaluru Hardware Park, Mahadeva, Kodigehalli, 562149 Bangalore North (India)
Dr. S. Verma
Shell International Exploration & Production Inc.
3333 Highway 6 South, 77082 Houston, TX (USA)

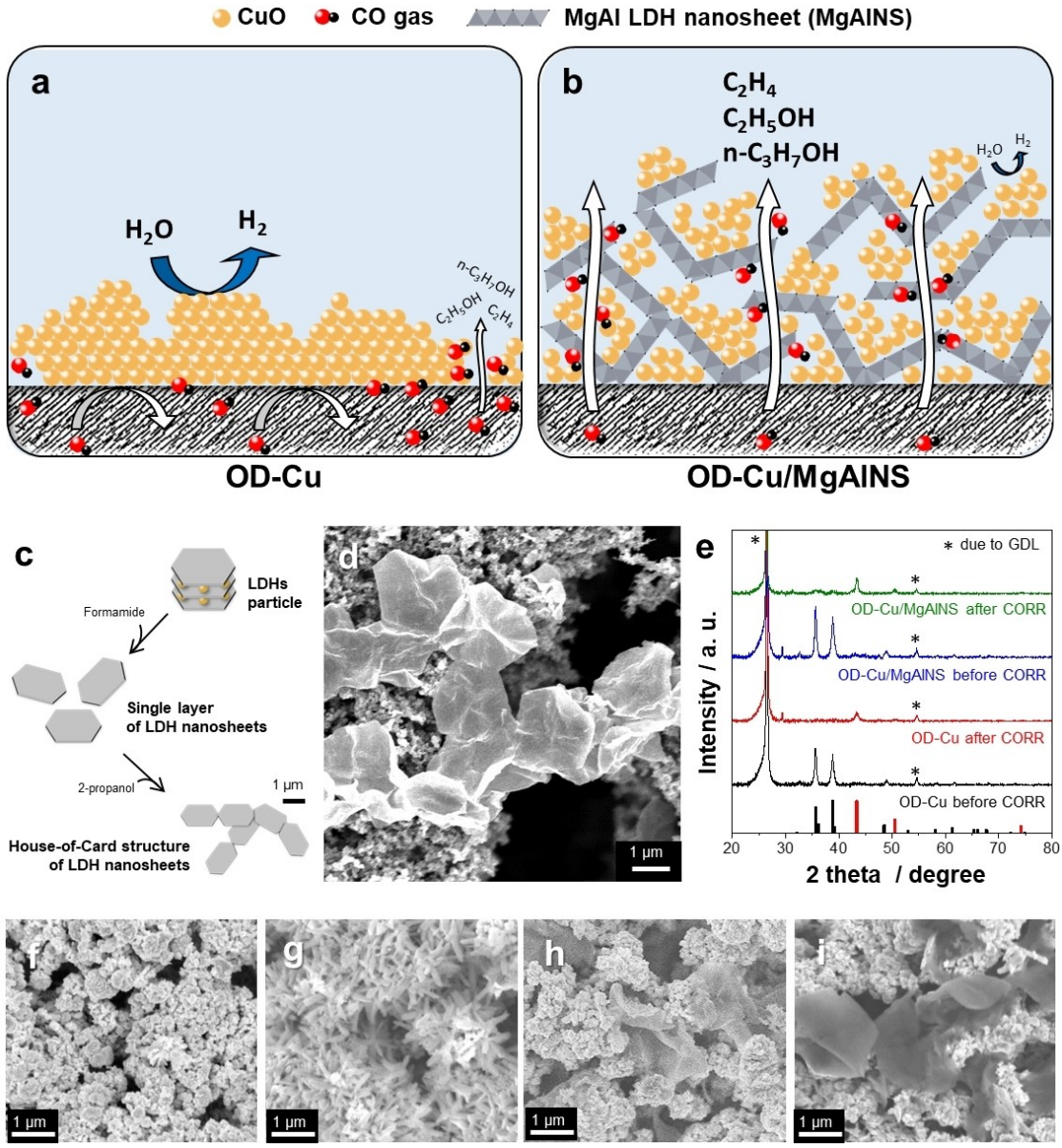

Figure 1. (a-b) Schematic illustration of catalysts loaded on gas diffusion layers during CORR: (a) OD-Cu only and (b) OD-Cu mixed with MgAl LDH nanosheets (MgAlNS). (c) Schematic representation of the formation of MgAl LDH nanosheet house-of-cards structures. (d) SEM image of MgAl LDH nanosheets, showing the house-of-cards structures. € XRD patterns of OD-Cu and OD-Cu/MgAlNS before and after they were used for CORR. Standard XRD patterns of CuO (black bars; Crystallography Open Database (COD) card number 1011194) and Cu (red bars; COD card number 4105681) are shown at the bottom of the figure. SEM images of OD-Cu (f) before and (g) after it was used as catalyst for CORR, and OD-Cu/MgAlNS (h) before and (i) after it was used as catalyst for CORR. The mass loadings of CuO and MgAlNS were respectively 2.91 and 0.29 mg cm^{-2}. We believed that in the absence of a support, the CuO particles were more agglomerated and thus reduced to aggregates of Cu^0 rods (Figure 1g) during CORR. In contrast, the MgAlNS dispersed the CuO particles well, which thus reduced the change in its morphology during CORR (Figure 1i).

reversible hydrogen electrode (RHE) with an average FE_{C2+} of 71 % and current density (j_{C2+}) of −1251 mA cm^{-2}. We show that the unique house-of-cards structure made by the LDH nanosheets disperses the Cu catalyst such that the *FE* of C_{2+} products can be maintained even with a high catalyst mass loading and at large overpotentials.

Results and Discussion

Characterization of OD-Cu/MgAlNS

The synthesis of the MgAl LDH and its exfoliation to nanosheets are presented in Figure 1c, Sections S1.1 and S2.[15] X-ray diffraction (XRD) and scanning electron microscopy (SEM) revealed that the MgAl LDH are crystalline and hexagonally shaped with lengths 1–2 μm (Figures S1 and

S2a). The exfoliated MgAl LDH nanosheets (MgAlNS) were first pre-assembled into a house-of-cards structure in solution (Figures 1d, S2b–S2d and S3).[17] They were then physically mixed with commercially-purchased CuO nanoparticles (< 50 nm, Sigma–Aldrich) in a mass ratio of 1:10, and used as CORR catalyst.

CuO (2.91 mg cm^{-2}) and CuO/MgAlNS catalysts (2.91 mg cm^{-2} CuO and 0.29 mg cm^{-2} MgAlNS) were respectively deposited onto carbon gas diffusion layers (GDL), and used as working electrodes in a flow cell electrolyzer. A Ag/AgCl reference electrode and a Ni foam counter electrode was used. Aqueous 1 M KOH served as electrolyte. A representative potential of −0.7 V vs. RHE (all potentials reported hereafter are referenced to the RHE) was applied for 1 hr. The CuO nanoparticles were reduced to aggregates of ~500 nm long Cu^0 rods (which we now termed as OD-Cu) after they were used as catalysts for CORR (Figure 1e–g). SEM imaging of the CuO/MgAlNS composite shows the MgAlNS dispersing the CuO nanoparticles (Figure 1h). After the composite was used as catalyst for CORR, the MgAlNS house-of-cards remained intact. More importantly, the dispersion of the now OD-Cu particles amongst the MgAlNS was preserved (Figures 1h–i and S6–7). We further found, using a tape test method, that the OD-Cu/MgAlNS film (after being used for CORR) was mechanically attached onto the GDL ~20 percentage points better, as compared to the unsupported OD-Cu (Section S3).[19]

Effects of House-of-Cards Scaffold on OD-Cu for CO Reduction

The effect of having a MgAlNS house-of-cards scaffold to support the OD-Cu during CORR is first studied using linear sweep voltammetry in 1 M KOH electrolyte (Figure S10). OD-Cu/MgAlNS showed a lower onset potential and higher total current density, compared to that of the unsupported OD-Cu. MgAlNS itself is electrochemically-inactive.

We next investigate the effects of various catalyst mass loadings on CORR at a representative potential of −0.7 V (Figure 2a–b, Tables S1 and S2; the potentials stated for all electrolyses have been iR-drop compensated). Mass loadings of CuO from 0.36 to 5.82 mg cm^{-2} were used. The major CORR products detected include ethylene, ethanol, 1-propanol and acetate (Figure S11). H_2 gas was formed from the hydrogen evolution reaction. Using an electrode loaded with 0.36 mg cm^{-2} of CuO, CO could be reduced to C_{2+} products with a *FE* of 70 %. When the CuO mass loading was increased to 0.73 and 1.46 mg cm^{-2}, the FE_{C2+} further increased to 72 and 73 %, respectively. However, at higher CuO mass loadings of 2.91 and 5.82 mg cm^{-2}, HER dominated, and the FE_{C2+} decreased to 20 and 19 %, respectively. The j_{C2+} also increased by only 2.4× from −37 to −90 mA cm^{-2}, as CuO mass loading increased. We attribute the decline in FE_{C2+} when higher mass loading was used to the catalyst particles aggregating, which lessens porosity within the catalyst layer and reduces the population of available active sites.[2,4,5]

When CuO particles physically mixed with MgAlNS (in a 1:10 mass ratio) were used as CORR catalysts, the *FE*s of C_{2+} products could be maintained at 62–72 %, even with the highest CuO mass loading of 5.82 mg cm^{-2} (Figure 2a; Table S2). More interestingly, we note that the j_{C2+} increased dramatically as the CuO/MgAlNS mass loadings increased (Figure 2b). Using 5.82 mg cm^{-2} of CuO mixed with 0.58 mg cm^{-2} MgAlNS, the average j_{C2+} obtained during CORR was −1251 mA cm^{-2}, which was 14-fold higher than that of using only CuO (−90 mA cm^{-2}). The partial current densities of ethylene and the C_{2+} alcohols were also remarkably high at −816 and −369 mA cm^{-2} respectively (compared with $j_{ethylene}$ = −27 mA cm^{-2} and j_{C2+} alcohols = −46 mA cm^{-2} exhibited by unsupported OD-Cu; Table S1). These results illustrate that the MgAlNS promote the formation of C_{2+} products even at high CuO mass loadings over 2 mg cm^{-2}. We highlight here that the MgAlNS themselves have negligible CORR catalytic activity, catalysing mainly H_2 evolution; the j_{total} exhibited by MgAlNS was only −0.3 mA cm^{-2} (Table S3).

We then compare the CORR activities exhibited by OD-Cu and OD-Cu/MgAlNS at potentials from −0.5 to −0.7 V (CuO loading: 2.91 mg cm^{-2} and MgAlNS loading: 0.29 mg cm^{-2}; Figure 2c–d, Tables S4–S5). It is again striking that by using a simple composite of MgAlNS physically mixed with CuO particles, CO could be sustainably reduced to C_{2+} products with *FE*s between 63–79 %. Over the same potential range, the j_{C2+} also increased ~12× from −79 to −908 mA cm^{-2}. In contrast, the FE_{C2+} exhibited by the unsupported OD-Cu decreased from 52 to 20 %, as the applied potential becomes more negative from −0.5 to −0.7 V. Their j_{C2+} were also low at between −17 to −61 mA cm^{-2}.

Carbon-based supports such as graphite and carbon nanotubes have been used to disperse catalyst particles and thereby increase their active catalytic areas.[20,21] However, these supports can alter, sometimes detrimentally, the intrinsic selectivities of the catalysts towards CO_2RR or CORR.[22] For example, multi-walled carbon nanotubes (MWCNT) loaded with Cu–Ni have been shown to promote hydrogen evolution, instead of CO_2 reduction.[22] Here in this study, we note that the relative selectivities of the various COR products formed did not change considerably whether OD-Cu or OD-Cu/MgAlNS catalysts were used. For example, during CORR at −0.7 V, the $FE_{ethanol}/FE_{ethylene}$ exhibited by OD-Cu and OD-Cu/MgAlNS were close at ~0.8 (Tables S1 and S2; loadings of CuO and MgAlNS were respectively 0.73 and 0.073 mg cm^{-2}). This observation indicates that the MgAlNS scaffolds do not affect the intrinsic catalytic activity of the OD-Cu.

The CORR activity and selectivity of our commercially-purchased CuO was further compared with that of highly CORR-active CuO nanoparticles synthesized using the procedure published by Jiao and co-workers (Figure S12 and Table S6).[4] At −0.7 V, the Cu catalyst synthesized using Jiao's method (which we shall termed as Cu_J) exhibited a j_{C2+} of −415 mA cm^{-2} and a FE_{C2+} of 65 %, which are significantly higher than that of the OD-Cu (j_{C2+} = −61 mA cm^{-2}; FE_{C2+} = 20 %). The enhanced performance

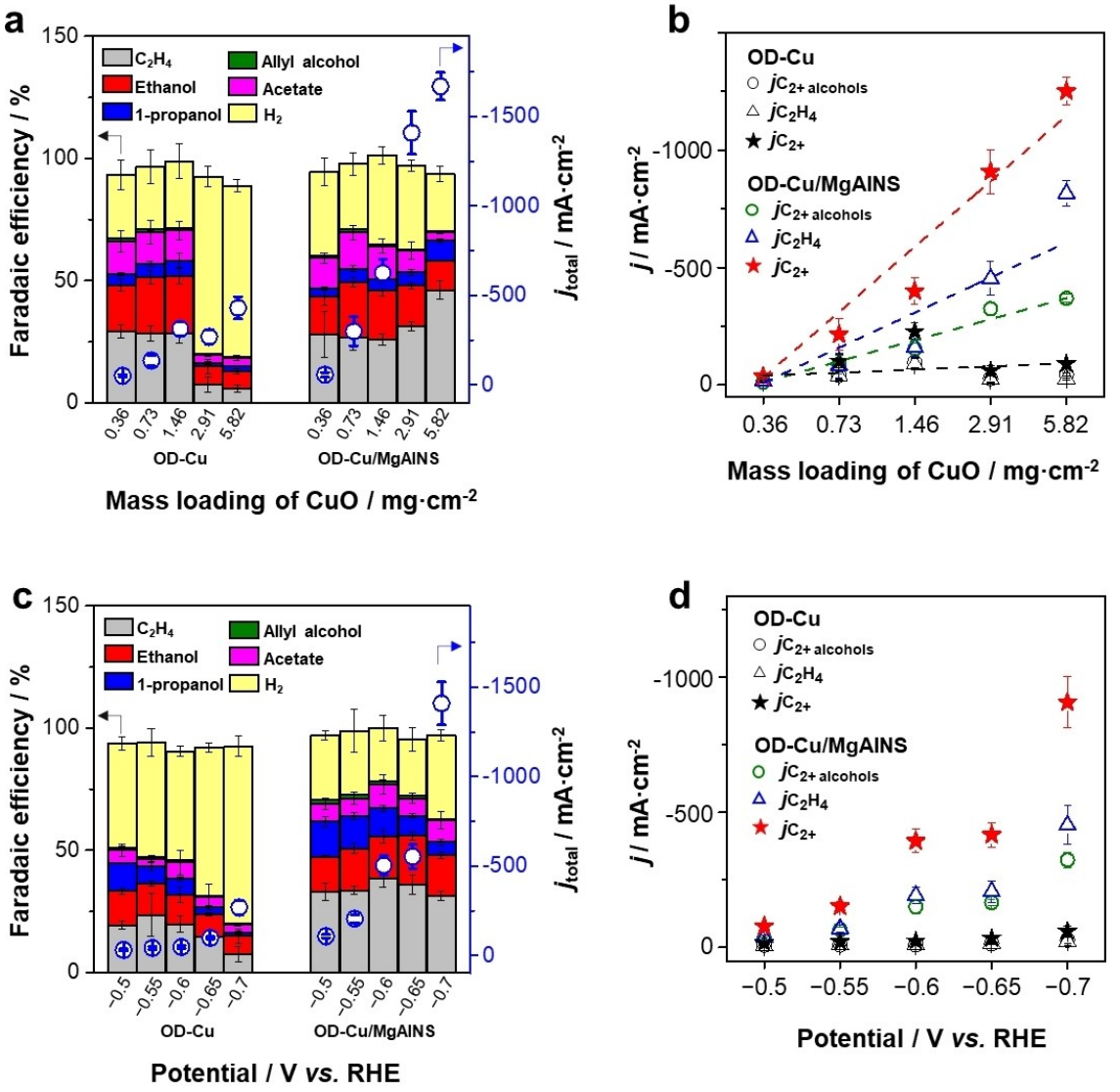

Figure 2. (a) Faradaic efficiencies and (b) partial current densities of major products formed during CORR at −0.7 V using various loadings of OD-Cu and OD-Cu/MgAlNS. The mass ratio of MgAlNS and CuO loaded on the GDL was always kept at 1 : 10. (c) Faradaic efficiencies and (d) partial current densities of major CORR products formed using OD-Cu and OD-Cu/MgAlNS at different applied potentials. The mass loadings of CuO and MgAlNS were respectively 2.91 and 0.29 mg cm^{-2}. Minor products with *FE*s less than 1 % are not shown in (a) and (c). Measurements were performed in a flow cell electrolyzer with 1 M KOH electrolyte.

of Cu_J has been attributed to its porous structure that facilitated rapid gas transport across the electrode-electrolyte interface. Interestingly, after mixing with MgAlNS, the performance disparity between these two catalysts became considerably bridged. Specifically, the FE_{C2+} of OD-Cu/MgAlNS and Cu_J/MgAlNS are now similar at 63–72 %, and their j_{C2+} range at −908 to −1195 mA cm^{-2}. Cu_J mixed with MgAlNS also appeared less aggregated as compared to the pure Cu_J (Figure S13a–d). This finding suggests that the careful dispersion of the electrocatalyst particles on the cathode is a more critical factor in determining its CORR activity and selectivity, rather than the original catalyst particle morphologies.[23]

Finally, at −0.7 V, the OD-Cu/MgAlNS catalyst could sustainably reduce, over 5 hr, CO to C_{2+} products with an average FE_{C2+} of 74 % and j_{C2+} of −1070 mA cm^{-2} (Figure S14). All in all, we demonstrate that OD-Cu supported on MgAlNS house-of-cards structures enabled larger CORR current densities and stable *FE*s to be obtained at high mass loadings and at more negative potentials.

Effect of MgAlNS on the CORR Performance of OD-Cu

The influence of the MgAlNS on the CORR performance of the OD-Cu was investigated. We first vary the amount of MgAlNS in the composite, while fixing the quantity of CuO to 2.91 mg cm^{-2} (Figure 3a and Table S7). Six mixtures were prepared. The partial current density of the C_{2+} products formed during CORR at −0.7 V increased dramatically

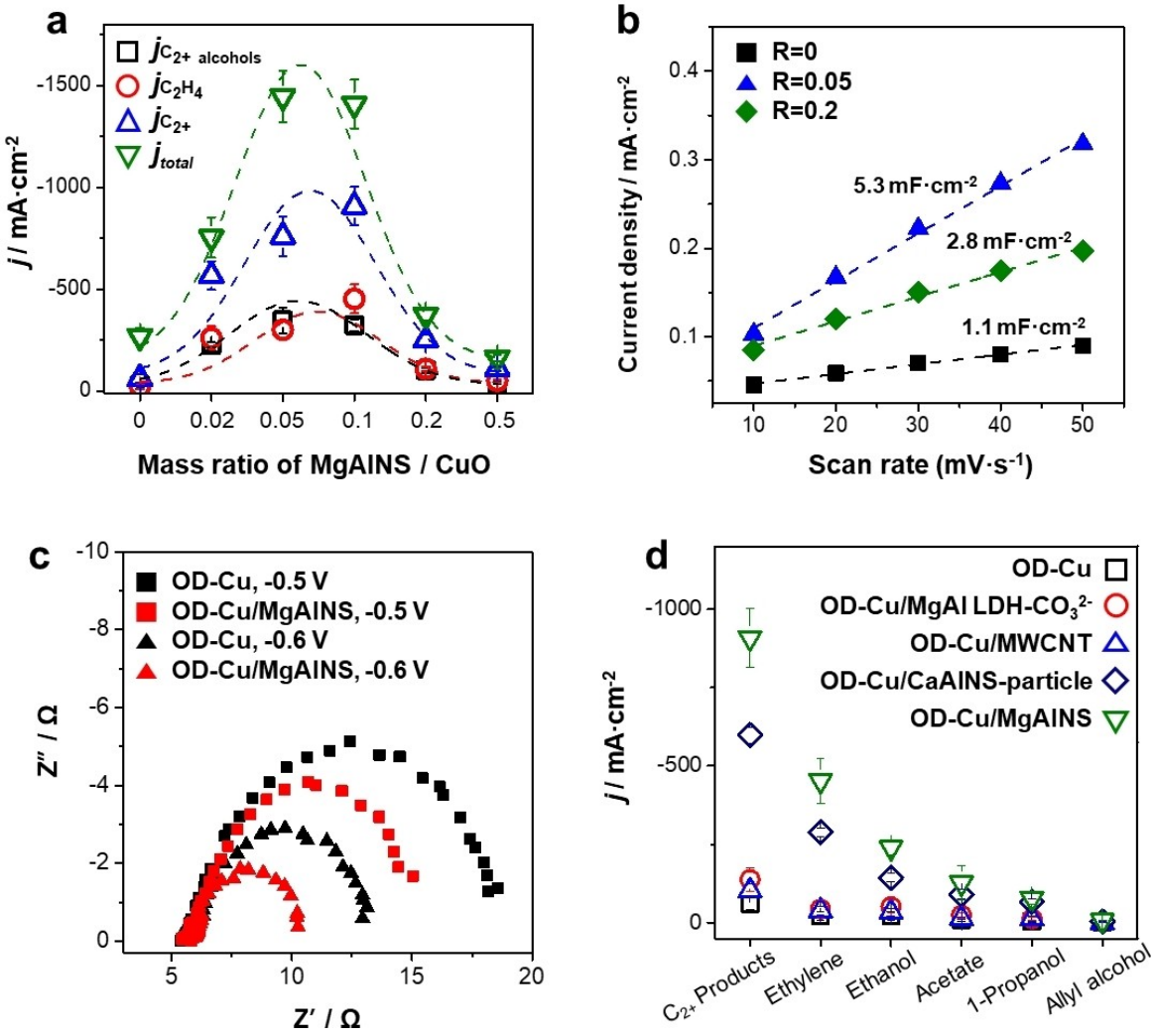

Figure 3. (a) Total current densities and partial current densities of C_{2+} products at −0.7 V vs. RHE formed during CORR using OD-Cu (CuO loading 2.91 mg cm^{-2}) mixed with different amounts of MgAlNS. The mass ratio or R is defined as the mass of MgAlNS loaded divided by that of CuO (2.91 mg cm^{-2}). (b) Double layer capacitance measurements of OD-Cu (CuO loading 2.91 mg cm^{-2}) mixed with different amounts of MgAlNS. The double-layer capacitances of samples with R = 0, 0.05 and 0.2 are shown in the figure. The measurements are made in N_2-saturated 1 M KOH electrolyte. (c) Nyquist plots of OD-Cu and OD-Cu/MgAlNS at −0.5 and −0.6 V vs. RHE in CO-saturated 1 M KOH electrolyte, respectively. The frequency range was from 10^5 Hz to 1 Hz. (d) Partial current densities of C_{2+} products formed during CORR at −0.7 V vs. RHE using OD-Cu, and OD-Cu mixed with MgAl LDH-CO_3^{2-}, MWCNT, CaAlNS-particle and MgAlNS. The mass ratios of the CuO and supports are kept at 10:1. CuO loading 2.91 mg cm^{-2}.

when a small amount of LDH nanosheet was added: from −61 mA cm^{-2} when $\frac{\text{Mass loading of MgAlNS}}{\text{Mass loading of CuO}} = R = \frac{0}{2.91} = 0$ to −568 mA cm^{-2} when R = 0.02. An optimized j_{C2+} value of −908 mA cm^{-2} could be achieved when the ratio of mass loadings of the MgAlNS to that of CuO was 0.1. Unexpectedly, upon further increasing the MgAlNS loading (R = 0.2 and 0.5), the current density of j_{C2+} decreased. We attribute this change to the aggregation of the LDH nanosheets into the LDH carbonate particles, as shown by XRD analysis (a peak at 11.7°; Figure S15).[14,18,24] Consequently, the OD-Cu catalysts would be less dispersed/more agglomerated. Following this line of reasoning, we would then expect the electrochemically-active surface areas (ECSAs) of the six catalyst composites to vary in a 'volcano'-like trend as the amount of LDH nanosheets added increases. We thus measured their double layer capacitances (which are proportional to their ECSAs) after they were used for CORR. A positive correlation between the current densities of C_{2+} products and double layer capacitances of the catalyst composites was indeed observed (Figures 3b and S16).

Electrochemical impedance spectroscopy (EIS) of the OD-Cu and OD-Cu/MgAlNS in CO-purged 1 M KOH electrolyte further showed that the charge transfer resistances (R_{ct}) of OD-Cu and OD-Cu/MgAlNS were similar at respectively 13.7 and 9.7 Ω at −0.5 V (7.7 and 4.6 Ω at −0.6 V) (Figure 3c). This confirms that the CORR charge transfer kinetics of the OD-Cu do not change considerably with the addition of the MgAlNS. These lines of evidences strongly suggest that the key role of the MgAlNS was to

optimally disperse the OD-Cu, thereby better exposing its catalytically-active sites to the CO feedstock.

Effects of other supports

To show the efficacy of the MgAlNS house-of-cards scaffold in enhancing the CORR activity of OD-Cu, we compare the current densities of C_{2+} products formed using catalyst composites consisting of 2.91 mg cm^{-2} CuO mixed with 0.29 mg cm^{-2} MgAl LDH-CO_3^{2-} particles, MWCNT or CaAl LDH nanosheets/particles (CaAlNS-particle) (Figures 3d, S17 and S18; Section S1.1). CO reduction was performed at −0.7 V in 1 M KOH electrolyte.

The j_{C2+} exhibited by OD-Cu/MgAl LDH-CO_3^{2-} and OD-Cu/MWCNTs were at −138 and −103 mA cm^{-2}, which were ~2× higher than that of pure OD-Cu (−61 mA cm^{-2}), but ~7–9× lower than that of OD-Cu/MgAlNS (−908 mA cm^{-2}). We further note that the FE_{H2} of OD-Cu/MgAl LDH-CO_3^{2-} was 38 %, which was lower than that (73 %) of OD-Cu (Table S8). These results implied that the LDH particle support do aid the mass transport of CO gas within the OD-Cu catalysts layer. However, they do not disperse the OD-Cu as well as the MgAlNS (FE_{H2} = 34 %), which thus account for their higher H_2 selectivity and lower j_{C2+}. With the use of MWCNT, HER dominated with a *FE* of 72 % (Table S8).

The average j_{C2+} exhibited by OD-Cu/CaAlNS-particle was at −598 mA cm^{-2}, which was ~4–10× higher than that of OD-Cu, OD-Cu/MgAl LDH-CO_3^{2-} and OD-Cu/MWCNT, but ~1.5× lower than that of OD-Cu/MgAlNS. We attribute this to the CaAl LDH-NO_3^- particles not being entirely exfoliated into nanosheets. Thus, less house-of-cards structures could be formed (Figures S18a-b and S19). Consequently, while this support does disperse OD-Cu, it did not do so as efficaciously as the MgAlNS.

In a broader context, by using OD-Cu/MgAlNS composite, we have shown that CO could be reduced to C_{2+} products with a j_{C2+} that is 14× higher than that of using unsupported OD-Cu (Figure 2a–b). The partial current density of C_{2+} alcohols could reach −369 mA cm^{-2}. These figures-of-merit compare favourably against those exhibited by Cu catalysts mixed with other supports (Figure 3d), and also those of Cu nanorods supported on nitrogen-doped carbon quantum dots (j_{C2+} alcohols of −147.8 mA cm^{-2} during CO_2RR at −0.9 V vs. RHE).[25] It is noteworthy that unlike many other supports, the MgAlNS scaffold is electrochemically inert and does not appear to alter the intrinsic catalytic activity of the OD-Cu. Its primary role is, instead, to promote CO gas flow through the OD-Cu catalyst layer. We thus believe that it can be applied as a general support for catalysts used in other (electro)catalytic reactions.

Conclusion

We have shown that MgAlNS house-of-cards scaffolds can serve as suitable supports for OD-Cu catalysts for CORR. Their use allow the rate of CO percolation through the catalyst layer to be enhanced, even when high mass loadings of catalysts and large overpotentials are applied. Consequently, CO reduction can be improved significantly, while H_2 evolution is minimized. Using this support-catalyst configuration, CO could be reduced to C_{2+} products with an average j_{C2+} of −1251 mA cm^{-2} at −0.7 V in 1 M KOH electrolyte. This j_{C2+} figure-of-merit is 14× higher compared to that exhibited by OD-Cu alone. The MgAlNS also aided in the mechanically stability of the catalyst layer on the GDL. Overall, we believe that the development of facilely-prepared Cu catalysts mixed with a MgAlNS house-of-cards support is a significant step towards the realization of industrial-scale CO reduction to multi-carbon products.

Experimental Section

Detailed experimental procedures can be found in Sections S1 and S3 of the Supporting Information.

Acknowledgements

The authors thank the National Research Foundation of Singapore (Urban Solutions and Sustainability, Industry Alignment Fund (Pre-Positioning) Programme, A-0004543-00-00), and Research & Experimentation group at Shell (A-0004543-01-00) for financial support of this project. The authors thank Prof. Jong Hyeon Lee from the Catholic University of Korea, department of chemistry, for useful scientific discussions.

Conflict of Interest

The authors declare no conflict of interest.

Data Availability Statement

The data that support the findings of this study are available from the corresponding author upon reasonable request.

Keywords: CO Electroreduction · Copper · Electrocatalysts · Layered Double Hydroxide Nanosheet

[1] Y. Zhou, A. J. Martín, F. Dattila, S. Xi, N. López, J. Pérez-Ramírez, B. S. Yeo, *Nat. Catal.* **2022**, *5*, 545–554.
[2] M. P. L. Kang, M. J. Kolb, F. Calle-Vallejo, B. S. Yeo, *Adv. Funct. Mater.* **2022**, *32*, 2111597.
[3] Y. Zhou, R. Ganganahalli, S. Verma, H. R. Tan, B. S. Yeo, *Angew. Chem. Int. Ed.* **2022**, *61*, e202202859; *Angew. Chem.* **2022**, *134*, e202202859.
[4] J. J. Lv, M. Jouny, W. Luc, W. Zhu, J. J. Zhu, F. Jiao, *Adv. Mater.* **2018**, *30*, 1803111.
[5] T. Möller, T. N. Thanh, X. Wang, W. Ju, Z. Jovanov, P. Strasser, *Energy Environ. Sci.* **2021**, *14*, 5995–6006.
[6] F. Pan, B. Li, E. Sarnello, S. Hwang, Y. Gang, X. Feng, X. Xiang, N. M. Adli, T. Li, D. Su, G. Wu, G. Wang, Y. Li, *Nano Energy* **2020**, *68*, 104384.

[7] H. Xu, D. Rebollar, H. He, L. Chong, Y. Liu, C. Liu, C.-J. Sun, T. Li, J. V. Muntean, R. E. Winans, D.-J. Liu, T. Xu, *Nat. Energy* **2020**, *5*, 623–632.
[8] T. Ma, Q. Fan, X. Li, J. Qiu, T. Wu, Z. Sun, *J. CO2 Util.* **2019**, *30*, 168–182.
[9] R. Ye, J. Dong, L. Wang, R. Mendoza-Cruz, Y. Li, P.-F. An, M. J. Yacamán, B. I. Yakobson, D. Chen, J. M. Tour, *Carbon* **2018**, *132*, 623–631.
[10] A. Ambrosi, S. Y. Chee, B. Khezri, R. D. Webster, Z. Sofer, M. Pumera, *Angew. Chem. Int. Ed.* **2012**, *51*, 500–503; *Angew. Chem.* **2012**, *124*, 515–518.
[11] Y. Lum, Y. Kwon, P. Lobaccaro, L. Chen, E. L. Clark, A. T. Bell, J. W. Ager, *ACS Catal.* **2016**, *6*, 202–209.
[12] A. I. Khan, D. O'Hare, *J. Mater. Chem.* **2002**, *12*, 3191–3198.
[13] A. Fogg, V. Green, H. Harvey, D. O'Hare, *Adv. Mater.* **1999**, *11*, 1466–1469.
[14] H. R. Cho, Y. M. Kwon, Y. J. Lee, Y. A. Park, H. G. Ji, J. H. Lee, *Appl. Clay Sci.* **2018**, *156*, 187–194.
[15] X. Xu, J. Wang, A. Zhou, S. Dong, K. Shi, B. Li, J. Han, D. O'Hare, *Nat. Commun.* **2021**, *12*, 3069.
[16] S. Kwon, H. T. Lee, J. H. Lee, *Eur. J. Chem.* **2020**, *26*, 14359–14365.
[17] J. A. Gursky, S. D. Blough, C. Luna, C. Gomez, A. N. Luevano, E. A. Gardner, *J. Am. Chem. Soc.* **2006**, *128*, 8376–8377.
[18] Y. Zhang, J. R. Evans, *Colloids Surf. A* **2012**, *408*, 71–78.
[19] ASTM Committee D01 (ASTM International), ASTM D3359-02, **2010**.
[20] N. Altaf, S. Liang, R. Iqbal, M. Hayat, T. R. Reina, Q. Wang, *J. CO2 Util.* **2020**, *40*, 101205.
[21] T. Möller, F. Scholten, T. N. Thanh, I. Sinev, J. Timoshenko, X. Wang, Z. Jovanov, M. Gliech, B. Roldan Cuenya, A. S. Varela, P. Strasser, *Angew. Chem. Int. Ed.* **2020**, *59*, 17974–17983; *Angew. Chem.* **2020**, *132*, 18130–18139.
[22] M. Wang, Z. Cai, B. Zhang, K. Yang, T. Shou, M. T. Bernards, P. Xie, Y. He, Y. Shi, *Energy Fuels* **2022**, *36*, 5833–5842.
[23] S. Nitopi, E. Bertheussen, S. B. Scott, X. Liu, A. K. Engstfeld, S. Horch, B. Seger, I. E. L. Stephens, K. Chan, C. Hahn, J. K. Nørskov, T. F. Jaramillo, I. Chorkendorff, *Chem. Rev.* **2019**, *119*, 7610–7672.
[24] P. Sahoo, S. Ishihara, K. Yamada, K. Deguchi, S. Ohki, M. Tansho, T. Shimizu, N. Eisaku, R. Sasai, J. Labuta, D. Ishikawa, J. P. Hill, K. Ariga, B. P. Bastakoti, Y. Yamauchi, N. Iyi, *ACS Appl. Mater. Interfaces* **2014**, *6*, 18352–18359.
[25] C. Chen, X. Yan, S. Liu, Y. Wu, Q. Wan, X. Sun, Q. Zhu, H. Liu, J. Ma, L. Zheng, H. Wu, B. Han, *Angew. Chem. Int. Ed.* **2020**, *59*, 16459–16464; *Angew. Chem.* **2020**, *132*, 16601–16606.

Manuscript received: November 23, 2022
Accepted manuscript online: February 16, 2023
Version of record online: March 8, 2023